Accurate and Efficient Modelling of Inelastic Hole-Acoustic Phonon Scattering in Monte Carlo Simulations

J.R. Watling[1], C. Riddet[1] and A. Asenov[1,2]
[1]Device Modelling Group, School of Engineering, University of Glasgow, Glasgow, G12 8LT, Scotland
[2]Gold Standard Simulations Ltd, The Rankine Building, Oakfield Avenue, Glasgow, G12 8LT, Scotland
Jeremy.Watling@glasgow.ac.uk

***Abstract* - Acoustic phonon scattering is known to play an important role in accurately describing hole-transport in semiconductors such as Si and Ge. However, it has been difficult to treat accurately and efficiently due to its dispersion relationship, thus it is often treated as an elastic process or by using constant phonon energy. Here we present an efficient approach for handling inelastic acoustic phonon scattering taking into account the full dispersion relationship. The proposed method unlike previous methods makes no assumption about the carrier distribution function, thus it is suitable for application within a device environment. The model is able to reproduce accurately the velocity-field characteristics over a wide-range of temperatures.**

Keywords: Acoustic Phonons, Monte Carlo

I. INTRODUCTION

The Monte Carlo (MC) algorithm has rapidly become a very powerful tool for providing numerical solutions for a wide variety of complex physical problems [1], such as the Boltzmann Transport (BTE) equation enabling the simulation of carrier transport in semiconductors [2].

However, for a MC simulator to provide an accurate solution of the BTE, it is necessary to provide physical models to describe efficiently both the bandstructure and the scattering mechanisms. Here a 6-band k•p model is employed, which allows for the incorporation of spin-orbit coupling and strain in a self-consistent way within the Hamiltonian [3], capturing the appropriate anisotropy of the valence bands and strain as applicable and illustrated in Fig. 1 for relaxed and strained Ge.

One of the most important intrinsic scattering mechanisms in the simulation of hole transport in Si and Ge are acoustic phonons, where the phonon energy is heavily dependent on the momentum transfer, q, which complicates matters. A frequently employed approximation is the elastic equi-partition approximation. However, this approximation is not well suited for the modelling of hole transport [4], as acoustic phonon scattering is important for accurate modelling of inter-band scattering between the light (LH) and heavy (HH) hole bands.

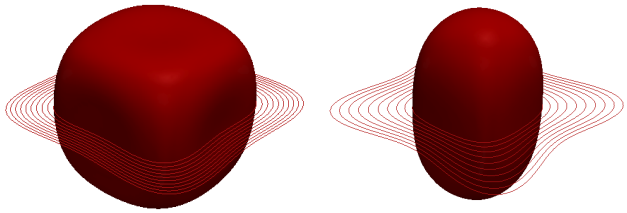

Fig. 1. Energy isosurface for the heavy hole band at 50meV for relaxed (left) and compressively strained (right) Ge (~2%) calculated using 6-band k•p.

One approach to overcome this limitation has been to take an average of the acoustic phonon energies and the corresponding momentum transfer [5]. This model demonstrates good agreement with experimental bulk velocity-field characteristics for a variety of temperatures. However, the averaging proposed relies on approximating the carrier distribution with a Maxwell-Boltzmann distribution with a well-defined carrier temperature. While this is sufficient for bulk, undoped simulations, it would be difficult within a device framework, where the carrier temperature can vary significantly throughout the device. The use of a Fermi-Dirac distribution, as required for modelling carrier transport within modern semiconductor devices [6], would require the averaging to be weighted by the probability that the final state is vacant, thus the averaged phonon energy obtained would be different for emission and absorption processes. An additional deficiency of this model is that due to an average momentum transfer being employed, the scattering rate no longer has a dependence on q. Previous studies [7,8] have noted that this can be an important effect in the warped valance bands of Si and Ge. The methodology we propose here overcomes all of these potential difficulties yet remains computationally efficient.

II. TREATEMENT OF INELASTIC ACOUSTIC PHONON SCATTERING

As commented previously, in the case of acoustic phonon scattering, the phonon energy is dependent on the momentum transfer. The scattering rate for acoustic phonon scattering within the Born approximation is given by:

$$\Gamma_{ac}\left(k,k'\right)=\frac{2\pi}{\hbar}\frac{V}{\left(2\pi\right)^3}\int_0^{\infty}k'^2dk'\int_0^{\pi}\sin\theta d\theta\int_0^{2\pi}d\phi \times\left|M\left(k,q\right)\right|^2\delta\left(E_{k'}-E_k\pm\hbar\omega_{\alpha}\left(q\right)\right) \tag{1}$$

Here the upper symbol denotes emission and lower absorption. The squared matrix element is in turn given by:

$$\left|M\left(k,q\right)\right|^2=\frac{\hbar\left(\Delta_{ac}^{\alpha}q\right)^2}{2\rho V\omega_{\alpha}\left(q\right)}\begin{pmatrix}N_q+1\\N_q\end{pmatrix}I_{k,k+q}^2 \tag{2}$$

where Δ_{ac}^{α} is the acoustic deformation potential for the particular acoustic mode α (longitudinal or transverse). N_q the Bose-Einstein phonon population and for the overlap integral $I_{k,k+q}^2$, the approximations of Wiley are employed [9]. The dispersion describing the relationship between the momentum transfer, q, and the phonon energy is given by:

$$\hbar\omega_{\alpha}\left(q\right)=\hbar\omega_{\max}^{\alpha}\left(\sin\left(\frac{qa}{4}\right)\right) \tag{3}$$

where the maximum phonon frequency for mode α is given by $\omega_{\max}^{\alpha}=4c^{\alpha}/a$, with c^{α} is the associated velocity of sound and a is the lattice constant of the material. The acoustic phonon velocities are obtained by taking an average over all crystallographic directions, obtained from a solution of the Christoffel equation [10], for each of the individual polarization modes, as shown in Fig. 2. This approach is justified, the averaged error being less than 5% for all modes.

The integrand in (1) is discontinuous requiring the determination of a self-consistent solution of the momentum q and energy constraints $\hbar\omega^{\alpha}(q)$ as given by:

$$k_f=k_i\pm q \tag{4}$$

$$E\left(k_f\right)=E\left(k_i\right)-\Delta E_{fi}\pm\hbar\omega^{\alpha}\left(q\right) \tag{5}$$

where i and f denote the initial and final states respectively and ΔE_{fi} the energy separation between initial and final states, assuming one exists.

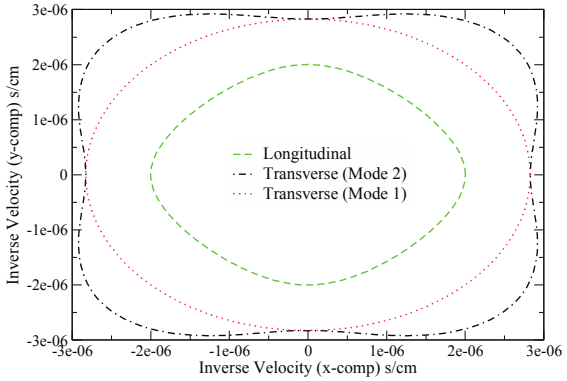

Fig. 2. Inverse velocities for different acoustic phonon modes in the *x-y* plane for relaxed Ge.

The integral described in (1) is not only time-consuming for both the determination of the scattering rate and the state after scattering, but the discontinuous nature of the integrand makes numerical integration unreliable. Our approach is to employ a change of variable to integration over *q,* thus the scattering rate is now given by:

$$\Gamma_{ac}(\mathbf{k})=\frac{\left(\Delta_{ac}^{\alpha}\right)^2}{4\pi\rho}\int\frac{\mathbf{q}^2}{\omega^{\alpha}\left(\mathbf{q}\right)\mathbf{k}\mathbf{k}'}\begin{pmatrix}N_q+1\\N_q\end{pmatrix}I_{k,k'}^2\mathbf{k}'^2 \times\left|\frac{d\mathbf{k}'}{dE\left(\mathbf{k}'\right)}\right|_{\mathbf{k}=\mathbf{k}'}\delta\left(E\left(\mathbf{k}'\right)-E\left(\mathbf{k}\right)\pm\hbar\omega^{\alpha}\left(\mathbf{q}\right)\right)d\mathbf{q} \tag{6}$$

The limits of integration on q taking into account both Normal and Umklapp processes are chosen to ensure conservation of energy and momentum combining (4) and (5). The integrand is now continuous within these limits, which can be pre-calculated for each initial state and stored for future use. In this framework a rejection technique is used to select the final state, where q is randomly selected within these limits previously determined and the energy exchange is given by (3). Our methodology satisfies the important requirement of detailed balance [11] and make no assumption about the carrier distribution, thus it is suitable for application within MC simulations of modern nano-scale devices.

III. RESULTS AND DISCUSSION

A. Calibration and verfication of simulator

The coupling constants for the phonon scattering mechanisms (acoustic and optical) have been calibrated to match experimental velocity-field data [11,12] for Si and Ge over a wide range of temperatures employing only a single set of parameters as shown in Figs. 3 and 4 respectively.

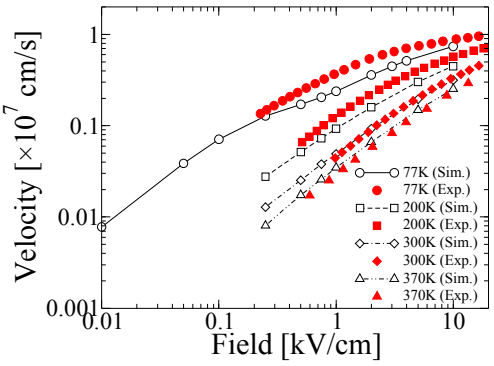

Fig. 3. Simulated velocity-field characteristics from 77K to 370K in relaxed, bulk Si, including only acoustic and optical phonon scattering compared to available experimental work.

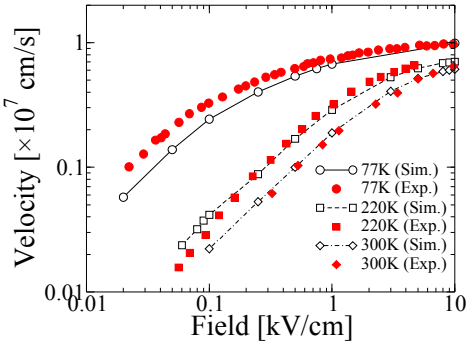

Fig. 4. Simulated velocity-field characteristics from 77K to 300K in relaxed, bulk Ge, including only acoustic and optical phonon scattering compared to available experimental work.

Inclusion of the complex anisotropic bandstructure obtained here through the use of a 6-band k•p approach along with an accurate description of the relevant scattering mechanisms is necessary to obtain good agreement over a wide range of temperatures and electric fields, as well to explain the complex interaction between channel and substrate in the presence of strain. This is illustrated in Fig. 5, where we present the hole mobility in undoped strained Ge layers for the three major substrate orientations: (001), (110) and (111), along with a variety of channel orientations, with (110) substrate coupled with $\langle \bar{1}10 \rangle$ channel direction demonstrating the highest mobility. In our previous work [13] we demonstrated that a general increase in mobility resulting from the application of strain was due to changes to the *E-k* relationship in different orientations.

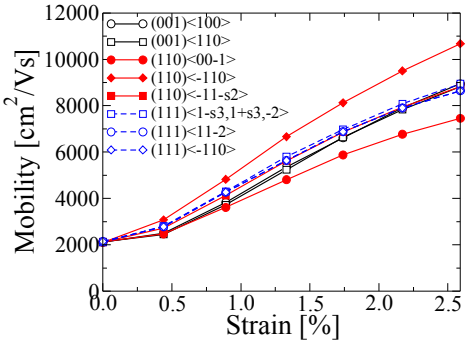

Fig. 5. Modelling in undoped Ge as a function of strain and orientation, illustrating the preferential combination to be $\langle \bar{1}10 \rangle(110)$.

B. Impact of Inelastic Acoustic Phonon Scattering

Mobility and HH band occupations as a function of biaxial strain in Ge and Si are illustrated in Figs. 6 and 7 respectively. This is for a $Si_{1-x}Ge_x$ substrate (applying compressive strain in Ge and tensile in Si), for a $\langle 110 \rangle$ channel orientation (this being the standard channel orientation employed with modern *p*-MOSFETs) on both (001) and (110) surfaces employing for comparison the equi-partition elastic approximation and the methodology for inelastic acoustic phonons described here. We observe that the difference between the inelastic and elastic phonon scattering decreases with temperature, as expected since the ratio $\hbar\omega(q)/k_BT$ decreases with temperature. Inelastic acoustic phonons have a greater effect for the (100) surfaces than (110) as the warped nature of the valence bands predominately favours a larger scattering angle for this surface orientation as compared to (110) as has been noted previously [7,8]. Tensile strain in Si causes the conductivity mass in the $\langle \bar{1}10 \rangle(110)$ case to increase, reducing the mobility, while compressive strain as in the case of strained Ge on a $Si_{1-x}Ge_x$ substrate causes a corresponding decrease. Additionally the strain induced band-spitting is greater in Si causing a larger discrepancy between the simulations using the different acoustic phonon scattering approaches, than in the case of Ge, as elastic phonon scattering obviously fails to accurately capture the inter-band acoustic phonon scattering in the presence of band splitting between the heavy and light hole bands. As a result the impact of inelastic acoustic phonons scattering is greatest at moderate values of strain, where the band-splitting is comparable to the acoustic phonon energy.

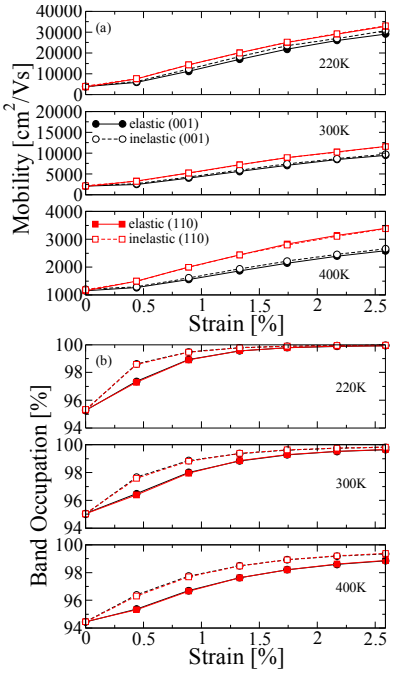

Fig. 6. (a) Mobility and (b) HH band occupation in compressively strained Ge for a ⟨110⟩ channel on (001) and (110) substrates, employing elastic and inelastic treatment for acoustic phonon scattering over a range of temperatures.

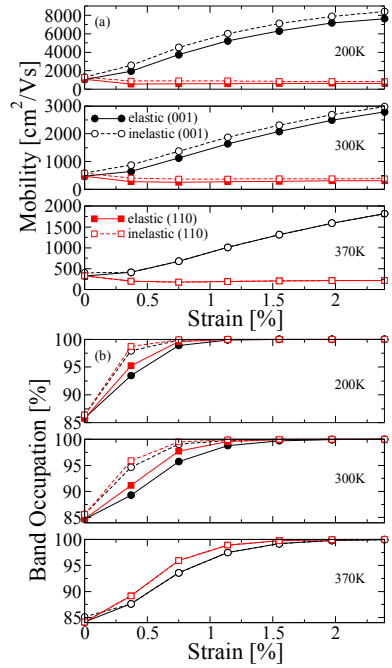

Fig. 7. (a) Mobility and (b) HH band occupation in tensile strained Si for a ⟨110⟩ channel on (001) and (110) substrates, employing elastic and inelastic treatment for acoustic phonon scattering over a range of temperatures.

IV. CONCLUSIONS

Ensemble Monte Carlo simulations have been carried out employing an efficient and accurate method for the inclusion of the full inelastic acoustic phonon dispersion curve.

We have studied the impact of inelastic acoustic phonon scattering on the hole mobility in relaxed and strained Si and Ge for a range of temperatures. It is observed that there is an anisotropic impact on the mobility due to the use of inelastic acoustic phonon scattering, with a greater impact observed for the (001) orientation due to the warped valence band structure. Tis is complemented by an increased impact with strain, due to the removal of the degeneracy of the heavy and light hole bands at the Γ point. Coupled with the observed differences between the elastic and inelastic simulations the above illustrates that inclusion of inelastic acoustic phonon scattering, is required for a complete accurate simulation of carrier mobilities in strained Si and Ge, even at moderate temperatures that might be encountered within the operation conditions of modern nano-scale devices.

REFERENCES

[1] R. W. Hockney and J. W. Eastwood, 'Computer Simulations using Particles', Taylor & Francis, (1998)

[2] M. V. Fischetti, "Monte Carlo Simulation of Transport in Technologically Significant Semiconductors of the Diamond and Zinc-Blende Structures - Part I: Homogeneous Transport," *IEEE Trans. Electron Devices*, vol. 38, pp. 634–649, March 1991.

[3] J. E. Dijkstra and W. T. Wenckebach, "Hole transport in strained Si," *Journal of Applied Physics*, vol. 81, pp. 1259–1263, February 1997.

[4] B. Fischer and K. R. Hofmann, "A full-band Monte Carlo model for the temperature dependence of electron and hole transport in silicon," *Appl. Phys. Lett.*, vol. 76, pp. 583–585, January 2000.

[5] F. M. Bufler, A. Schenk, and W. Fichtner, "Simplified model for inelastic acoustic phonon scattering of holes in Si and Ge," *J. Appl. Phys.*, vol. 90, pp. 2626–2628, September 2001.

[6] J. R. Watling, C. Riddet, M. K. H. Chan, and A. Asenov, "Simulation of hole-mobility in doped relaxed and strained Ge layers," *J. Appl. Phys.*, vol. 108, p. 093715, 2010.

[7] M. Tiersten, "Acoustic-mode scattering mobility of holes in diamond type semiconductors," *J. Phys. Chem. Solids*, vol. 25, pp. 1151-1168, November 1964.

[8] F. L. Madarasz and F. Szmulowicz, "Transition rates for acoustic-phonon - hole scattering in p-type silicon with nonparabolic bands," *Phys.l Rev. B*, vol. 24, pp. 4611–4622, October 1981

[9] J. D. Wiley, "Polar Mobility of Holes in III-V Compounds," *Phys. Rev. B*, vol. 4, pp. 2485–2493, October 1971.

[10] A. G. Every, "General closed-form expressions for acoustic waves in elastically anisotropic solids," *Phys. Rev. B*, vol. 22, pp. 1746-1760, 1980.

[11] F. Reif, 'Fundamentals of Statistical and Thermal Physics', McGraw-Hill Book Company, New York (USA), (1985)

[12] L. Reggiani, C. Canali, F. Nava, and G. Ottaviani, "Hole drift velocity in germanium," *Phys. Rev. B*, vol. 16, pp. 2781–2791, September 1977.

[13] J. P. Nougier and M. Rolland, "Mobility, Noise Temperature, and Diffusivity of Hot Holes in Germanium," *Phys. Rev. B*, vol. 8, pp. 5728–5737, December 1973.

[14] C. Riddet *et al.*, "Hole Mobility in Germanium as a Function of Substrate and Channel Orientation, Strain, Doping, and Temperature," *IEEE Trans. Electron Devices,* in press.